

Superconducting-Spin Reorientation in Spin-Triplet Multiple Superconducting Phases of UTe₂

Katsuki Kinjo^{1*†}, Hiroki Fujibayashi¹, Hiroki Matsumura¹, Fumiya Hori¹, Shunsaku Kitagawa¹,
Kenji Ishida^{1*}, Yo Tokunaga², Hironori Sakai², Shinsaku Kambe², Ai Nakamura³,
Yusei Shimizu³, Yoshiya Homma³, Dexin Li³, Fuminori Honda^{3,4}, and Dai Aoki^{3,5}

¹Department of Physics, Graduate School of Science, Kyoto University; Kyoto, Kyoto, 605-0953, Japan.

²Advanced Science Research Center, Japan Atomic Energy Agency; Tokai, Ibaraki, 319-1195, Japan.

³Institute for Materials Research, Tohoku University, Oarai, Ibaraki, 311-1313, Japan

⁴Central Institute of Radioisotope Science and Safety, Kyushu University, Fukuoka, 819-0395, Japan

⁵University Grenoble Alpes, CEA, Grenoble INP, IRIG, PHELIQS; F-38000 Grenoble, France

[†]Present address: Institute of Multidisciplinary Research for Advanced Materials, Tohoku University, Sendai, Miyagi, 980-8577, Japan

*Corresponding author. Email: katsuki.kinjo.c6@tohoku.ac.jp (K.K.); kishida@scphys.kyoto-u.ac.jp (K.I.).

Abstract: Superconducting (SC) state has spin and orbital degrees of freedom, and spin-triplet superconductivity shows multiple SC phases due to the presence of these degrees of freedom. However, the observation of spin-direction rotation occurring inside the SC state (SC spin rotation) has hardly been reported. UTe₂, a recently discovered topological superconductor, exhibits various SC phases under pressure: SC state at ambient pressure (SC1), high-temperature SC state above 0.5 GPa (SC2), and low-temperature SC state above 0.5 GPa (SC3). We performed nuclear magnetic resonance and AC susceptibility measurements on single-crystal UTe₂. The *b*-axis spin susceptibility remains unchanged in SC2, unlike in SC1, and decreases below the SC2-SC3 transition with spin modulation. These unique properties in SC3 arise from the coexistence of two SC order parameters. Our NMR results confirm the spin-triplet superconductivity with SC spin parallel to *b* in SC2, and unveil the remaining of spin degrees of freedom in superconducting UTe₂.

One-Sentence Summary: Multiple superconducting phases with spin rotation in the superconducting state was observed.

Introduction

What kind of an ordered state is realized under competing interaction is a central issue in condensed matter physics. Superconductivity and superfluidity are most remarkable macroscopic quantum phenomena produced by two-fermion pairs, so-called the Cooper pair. In conventional superconductivity, which covers almost all superconductors discovered so far, the Cooper pairs have zero total spin and orbital angular momenta, and have no degrees of freedom. Therefore, only one superconducting (SC) state is realized.

Theoretically, it is possible that either or both of the two angular momenta are non-zero, and hence the coexistence of two SC phases, and/or multiple SC phases was anticipated. The well-known example of such multi-phases is superfluid ^3He , in which two phases (A and B) with lowest energy are realized in zero field, and becomes more complex under magnetic fields and/or anisotropic environment (1-4). The presence of the Majorana particles, which is applicable to “qubits” in quantum computer was suggested in the surface state of the B phase (5). However, in superconductors, there are only limited examples for such multiple SC phases, for example, UPt_3 (6), Th-doped UBe_{13} (7), and CeRh_2As_2 (8) are known so far. In addition, SC-spin rotation, which is the smoking gun for the spin-triplet SC multiphase due to the presence of the spin degrees of freedom, has hardly been observed, because of the tiny difference between the two critical temperatures (9). It is quite important to find the textbook examples of the spin triplet superconductivity, corresponding to the superfluid ^3He , and to find the phenomena related to the spin and orbital degrees of freedom.

Herein, we focus on a recently discovered uranium-based superconductor uranium ditelluride (UTe_2) with SC transition temperature $T_c \sim 1.6$ K (10). UTe_2 , crystallizing orthorhombic structure with space group $Immm$ (#71, D_{2h}), as shown in Fig. 1A, has the multiple SC phases. Under pressure (P), the T_c of UTe_2 increases to about 3 K at 1.2 GPa (11-13), as shown in Fig. 1B. Below 1.6 GPa, the two jumps in the temperature (T) dependence of specific heat indicate the existence of at least two SC phases (11, 13): one exists at ambient pressure (SC1) and its T_c gradually decreases with applying P , and the other is an SC phase induced by P above 0.5 GPa (SC2), whose T_c has a maximum at 1.2 GPa. As a result, T_c of SC1 is below T_c of SC2 above 0.5 GPa, and thus we call this SC state SC3 in this paper. Above 1.6 GPa, superconductivity suddenly disappears and a magnetic anomaly, which is considered as the antiferromagnetic state, was observed (13).

In addition, UTe_2 shows multiple SC phases even at ambient pressure. For $H \parallel b$, T_c first decreases with increasing H and shows a minimum at around 16 T, then T_c increases up to 35 T (14). The bulk SC properties in the high-field (HF) SC phase were recently confirmed by thermodynamic and χ_{AC} measurements (15, 16), suggesting that the pairing interaction grows up above 16 T (15).

Furthermore, recent nuclear magnetic resonance (NMR) measurements revealed a tiny change of spin susceptibility just below T_c for $H \parallel b$ and $H \parallel c$ (17-19), and almost no change in the a -axis spin susceptibility (20). Above 14 T for $H \parallel b$, spin susceptibility remains constant below T_c (16, 18). These results indicate that UTe_2 is a spin-triplet superconductor with the spin degrees of freedom and the SC order parameter \mathbf{d} -vector, which is perpendicular to the SC spin, having the b and c components in the low-field (LF) region. In UTe_2 , a complex interplay of various interactions was reported, such as Ising-like ferromagnetic fluctuations from NMR studies (21) and the antiferromagnetic fluctuations from the inelastic neutron scattering measurements (22, 23). Such competing interactions are thought to induce rich physics such as the HFSC phase in $H \parallel b$

and multiple SC phases under pressure. Thus, identifying the SC properties of the SC2 and SC3 states is the last piece to understanding the multiple SC phases of UTe_2 .

To elucidate the SC properties of the multiple SC phases in UTe_2 , nuclear magnetic resonance (NMR) serves as a highly effective tool. NMR is a technique that probes nuclear spins, which interact with electron spins through strong hyperfine interactions. Consequently, it enables us to investigate the electron spin susceptibility microscopically. While the spin susceptibility in the SC state cannot be measured due to the SC diamagnetism by the bulk magnetization measurement, NMR can detect it with the hyperfine interaction. Moreover, to measure spin susceptibility in the multiple SC states under pressure, NMR is a unique measurement that meets these requirements.

Here, we report the results of the NMR Knight shift K for $H \parallel b$ (K_b) at 1.2 GPa, at which T_c of SC2 is maximum. We found that the spin susceptibility along the b axis is unchanged in SC2, which is different from that observed in SC1 at ambient pressure. More surprisingly, at the SC2-SC3 transition, K_b suddenly decreases and the NMR-spectral width becomes broader. These results suggest that the SC order parameter of SC1 and SC2 is different and that SC2 is a spin-triplet superconductivity with spin oriented toward the b axis and SC spin reoriented in SC3 state. These results suggest that the SC order parameter \mathbf{d} -vector was changed at the SC3 transition, and the spin degrees of freedom remains in the superconductivity of UTe_2 .

Results and Discussion

As there are two crystallographically inequivalent Te sites in UTe_2 , we observed two ^{125}Te -NMR peaks as reported in the previous paper (17–19). An NMR peak with the smaller [larger] K in $H \parallel b$ as Te(1) [Te(2)] by following the previous paper (21). The T variation of the NMR spectrum of Te(2) at $P = 1.2$ GPa is shown in the Fig. 2A, and the T dependence of the full width at half maximum (FWHM), the NMR Knight shift (K) determined with the NMR spectrum, and χ_{AC} are shown in Fig. 2B. Here, the NMR Knight shift is proportional to the spin susceptibility and the FWHM is proportional to the distribution of magnetization. As reported in the previous paper (24–26), K_b exhibits a broad maximum at $T\chi_{\max}$ and gradually decreases with decreasing T , similar to the T dependence of χ (24). Owing to the increase in T_c and the decrease in $T\chi_{\max}$ with increasing P (24), K_b highly depends on T around T_c at 1.2 GPa, unlike the case of ambient pressure (0 GPa). To clarify the change in the Knight shift related to the SC transition, we calculate $\Delta K \equiv K_{\text{SC}}^{\text{spin}} - K_{\text{normal}}^{\text{spin}}$ as shown in Fig. 3A. Here, $K_{\text{normal}}^{\text{spin}}$ ($K_{\text{SC}}^{\text{spin}}$) is K^{spin} in the normal (SC) state, and is estimated from the extrapolation above T_c . Although the absolute value of the spin part in K (K_{spin}) decreases with decreasing T , ΔK is almost zero above 0.5 K, indicating that the spin susceptibility in SC2 is the same as that in the normal state for $H \parallel b$. This T dependence of the spin susceptibility in SC2 is similar to that in the A phase of the ^3He superfluid (27). Below 0.5 K, we observed a sudden decrease in K_b and a broadening of the NMR spectrum, although no additional change was observed in χ_{AC} . The magnitude of the decrease in K_b below 0.5 K is almost the same as that in K at 0 GPa (17). This is further evidence of the occurrence of the phase transition inside the SC state from the microscopic point of view.

Now, we consider possible SC order parameters suggested by the present NMR results. As discussed in the previous papers (17–20), the order parameter of spin-triplet superconductivity is \mathbf{d} -vector, which is perpendicular to the SC spin components. In other words, K_i proportional to the spin susceptibility along the i axis decreases when \mathbf{d} -vector has the i component, but is unchanged

when the \mathbf{d} -vector has no i component. This corresponds to the SC spin pointing to the i direction. The possible SC phases at zero field are listed in Table 1 of Ref. (16). Our findings indicate that the \mathbf{d} -vector has no b component (the SC-spin is oriented to the b axis) in SC2, and has a finite b component in SC3, which is the same as that of SC1. This is the \mathbf{d} -vector rotation, evidencing the spin-triplet multiple SC phases with spin-degrees of freedom.

Another important point of Fig. 2B is that the FWHM of the Te(2) site shows an additional increase below 0.5 K. Figures 3A, 3B, and 3C show the temperature dependence of the FWHM divided by the applied fields ($\mu_0 H$), which reflects the distribution of the spin-susceptibility, ΔK measured at the Te(2) site, and χ_{AC} measured at 0.8, 1.0, and 2.5 T, respectively. To clarify the increase in line width due to the normal-SC2 transition and the increase in line width due to the SC2-SC3 transition, we defined the values $\Delta\text{FWHM}^{\text{Meissner}}$ and $\Delta\text{FWHM}^{\text{SC-SC}}$. $\Delta\text{FWHM}^{\text{Meissner}}$ and $\Delta\text{FWHM}^{\text{SC-SC}}$ are defined as $\text{FWHM}(\text{SC2}) - \text{FWHM}(\text{Normal})$ and $\text{FWHM}(\text{SC3}) - \text{FWHM}(\text{SC2})$, respectively, as shown in Fig. 3D. In general, the FWHM of the NMR spectrum increases below T_c due to SC diamagnetism. This effect is related to the SC penetration depth and was observed below 3.0 K in SC2, and was suppressed with increasing $\mu_0 H$, as shown in Fig. 3E. Decrease of $\Delta\text{FWHM}^{\text{Meissner}}/\mu_0 H$ with applying H is interpreted by the conventional SC diamagnetic effect. However, the additional increase in the FWHM below 0.5 K ($\Delta\text{FWHM}^{\text{SC-SC}}/\mu_0 H$) cannot be explained by such SC diamagnetic effect, since χ_{AC} shows no anomaly around 0.5 K, and $\Delta\text{FWHM}^{\text{SC-SC}}/\mu_0 H$ is independent of the applied field, as shown in Fig. 3F. In addition, from the comparison of the NMR spectra between 0.6 K (SC2) and 0.13 K (SC3), it is noted that the spectrum shows a tail to the larger Knight-shift side than the Knight shift in SC2 as shown in Fig. 4A. This is quite unusual for the NMR spectrum in the SC state, as the spin susceptibility decreases in the SC state. Such an NMR spectrum variation in the SC state was not observed in SC1 [Fig. 4 (A)], although the spectrum broadening due to the SC diamagnetic effect was observed. The ratio between the FWHM of the Te(1) and Te(2) spectra in SC3 is almost unchanged to that in the normal state (28). These results indicate that the additional linewidth broadening in SC3 arises from the unusual inhomogeneity of the spin susceptibility, which was not observed in SC1. Thus, SC3 is a different SC state from SC1.

We consider the several possibilities of the origin of linewidth broadening in SC3. One is due to the SC vortex state in SC3. Since spin susceptibility is unchanged in SC2, the NMR signal from the vortex core is observed at almost the same position as the SC NMR signal outside the vortex. On the other hand, the spin susceptibility decreases in SC3, and the signal from the vortex core should be observed at the different position from the SC NMR signal, resulting in the NMR signal becoming broader in the mixed state of SC3. However, this possibility would be unlikely, because the measurement fields are far below $H_{c2}^{\text{orb}} \sim 70$ T expected from Werthamer, Helfand, and Hohenberg (WHH) theory (29). Thus, the area fraction of vortex is approximately 1%, and the contribution to the NMR spectrum is negligibly small. Another possibility is the spatial inhomogeneity with coexistence of the two SC states in the sample. However, this possibility is ruled out, as the observed spectra could not be explained by the simple coexistence of the SC2 and SC3 states (28). These results indicate that, whatever the inhomogeneities in the sample, the NMR linewidth broadening intrinsically occurs below the SC2-SC3 transition, and is proportional to the magnetic field. In other words, it represents an increase in the distribution of the magnetic susceptibility in the SC3 state. At present we have no clear interpretation of this phenomenon, but we believe that we observed an effect due to the mixing of the two SC order parameters as in the case of (U,Th)Be₁₃ (30, 31). Actually, it was pointed out that the nonunitary spin triplet superconductivity leads to a spin-density wave type modulation of \mathbf{d} -vector from the theoretical studies (32).

Figures 5A and 5B shows the schematic image of the T vs H along the b axis (H_b) phase diagram of UTe_2 at ambient pressure (A) and 1.2 GPa (B), respectively (13, 15, 18, 26). At ambient pressure, $T_c(H)$ decreases in the LFSC (Low field superconducting) state, and increases in the HFSC (High field superconducting) state up to the metamagnetic field 35 T (H_m). In the LFSC state, K_b slightly decreases below T_c (17) (see Fig. 5B). As mentioned above, K_b is unchanged in the HFSC state (16) as shown in Fig. 5C, indicating that the SC spin align to the b axis. At the pressure ~ 1.2 GPa where T_c becomes maximum, H_m is suppressed to almost half of H_m at $P = 0$ and there is no more L-shape behavior in H_b - T phase diagram (26). Considering the similarity in spin susceptibility in the SC state between the HFSC and SC2 states and first order transition like disappearance of SC state and Kondo coherent state with applying field or pressure (25, 33, 34), we conclude that the HFSC evolves into SC2 with applying pressure. In addition, the SC1 phase hides under the SC2 phase and becomes the SC3 phase (coexisting phase of SC1 and SC2), while the SC3 phase appears only inside the SC2 phase.

Another similarity between HFSC and SC2 is that T_c increases with increasing K_b ; Figure 6 shows the values of K_b under magnetic field or under pressure. When a magnetic field is applied, the zero-field extrapolated T_c continues to increase with the application of the field (34), and K_b also increases. This tendency was also observed in the pressure experiment. When K_b is above 6.0 %, indicating the sample in SC2, T_c increases up to 3 K with increasing K_b . The T_c vs K_b curves show similarity between under pressure and under magnetic field. It strongly suggests that HFSC and SC2 are the similar phase and have the same origin. Based on this scenario, we suggest that the spin susceptibility along the b axis (χ_b) is an important parameter for HFSC and SC2, which determine the T_c of these states.

In conclusion, we have performed ^{125}Te -NMR measurement on UTe_2 under pressure to investigate the SC properties and determine the SC order parameter of SC2 and SC3 phases. The b -axis spin susceptibility in SC2 has the same value as that of the normal state below 3.0 K above 0.5 K. Below 0.5 K, spin susceptibility decreases, and the NMR linewidth increases. These results indicate that the SC order parameter is changed, *i.e.*, SC spin rotation occurs at the SC2-SC3 transition, and the novel SC state with two SC order parameters in SC3. This is microscopic evidence for the remaining the spin-degrees of freedom in the superconductivity of UTe_2 , inherent to the spin-triplet superconductivity.

Materials and Methods

Sample Preparation

A high-quality single-crystal UTe_2 sample was grown by the chemical vapor transport method with Iodine as a transport agent, details of which are described in ref. (10, 36). The single crystal of UTe_2 was an almost rectangular shape with $2 \times 1 \times 1 \text{ mm}^3$, with 2 mm along the a axis. To improve ^{125}Te -NMR signal intensity, the sample was synthesized with the ^{125}Te -enriched (99.9 %) metal as discussed in ref. (18). The transition temperature (T_c) of this sample is 1.6 K at ambient pressure.

AC susceptibility measurements

In order to confirm T_c , we measured the high-frequency AC susceptibility χ_{AC} using the NMR tank circuit. In the superconducting state, the impedance of the circuit changes due to the Meissner effect, and thus the tuning frequency of the circuit drastically changes just below T_c .

Applying pressure and pressure estimation

The hydrostatic pressure is applied using a piston-cylinder-type cell made of NiCrAl and CuBe alloys as described in ref. (37). Daphne 7373 was used as a pressure medium. The applied pressure was estimated by the SC transition temperature of Pb with the formula of $P = (7.181 - T_c(P))/0.364$ (38).

Field Alignment

We used a split-pair magnet to apply horizontal fields to the sample and a ^3He - ^4He dilution refrigerator that can be rotated about the vertical axis. With this setup, we could rotate the magnetic field direction within the bc plane of the sample. The direction of the magnetic field was confirmed by measuring the Te1 signal as described in ref. (24).

NMR measurements

An NMR spectrometer with a 100 W (at 0 dB input) power amplifier (Thamway Product: N146- 5049A) was used for the measurements. A conventional spin-echo method was used for NMR measurements in the temperature range from 0.1 to 4.2 K and in the magnetic field range from 0.8 to 2.5 T. All measurements were carried out with the ^3He - ^4He dilution refrigerator, in which the pressure cell was immersed into the ^3He - ^4He mixture to reduce radio frequency heating during measurements. The NMR spectrum was obtained by summation of the FFT spectrum with a 5 kHz step. The applied field is estimated by ^{65}Cu -NMR measurements as discussed here (39).

References and Notes

- (1) A. J. Leggett, A theoretical description of the new phases of liquid ^3He , *Rev. Mod. Phys.* **47**, 331-415 (1975).
- (2) J. C. Wheatly, Experimental properties of superfluid ^3He , *Rev. Mod. Phys.* **47**, 415-470 (1975).
- (3) H. Kojima, H. Ishimoto, Spin Polarized Superfluid ^3He A₁, *J. Phys. Soc. Jpn.* **77**, 111001 (2008).
- (4) V. V. Dmitriev, M. S. Kutuzov, A. A. Soldatov, A. N. Yudin, Superfluid β phase of ^3He , *Phys. Rev. Lett.* **127**, 265301 (2021).
- (5) S. Murakawa, Y. wada, Y. Tamura, M. Wasai, M. Saitoh, Y. Aoki, R. Nomura, Y. Okuda, Y. Nagato, M. Yamamoto, S. Higashitani, K. Nagai, Surface Majorana Cone of the Superfluid ^3He B Phase, *J. Phys. Soc. Jpn.* **80**, 013602 (2011).
- (6) R. Joynt, L. Taillefer, The superconducting phases of UPt_3 , *Rev. Mod. Phys.* **74**, 235-294 (2002).
- (7) G. R. Stewart, UBe_{13} and $\text{U}_{1-x}\text{Th}_x\text{Be}_{13}$: unconventional superconductors. *J. Low Temp. Phys.* **195**, 1-25 (2019).
- (8) S. Khim, J. F. Landaeta, N. Bannor, M. Brando, P. M. R. Brydon, R. Cardoso-Gil, U. Stockert, A. P. Mackenzie, D. F. Agterberg, C. Geibel, E. Hassinger, Field-induced transition within the superconducting state of CeRh_2As_2 , *Science* **373**, 1012-1016 (2021).
- (9) H. Tou, Y. Kitaoka, K. Ishida, K. Asayama, N. Kimura, Y. Onuki, E. Yamamoto, Y. Haga, and K. Maezawa, Nonunitary Spin-Triplet Superconductivity in UPt_3 : Evidence from ^{195}Pt Knight Shift Study, *Phys. Rev. Lett.* **80**, 3129-3132 (1998).
- (10) S. Ran, C. Eckberg, Q.-P. Ding, Y. Furukawa, T. Metz, S. R. Saha, I.-L. Liu, M. Zic, H. Kim, J. Paglione, N. P. Butch, Nearly ferromagnetic spin-triplet superconductivity, *Science* **365**, 684-687 (2019).
- (11) D. Braithwait, M. Vališka, G. Knebel, G. Lapertot, J.-P. Brison, A. Pourret, M. E. Zhitomirsky, J. Flouquet, F. Honda, D. Aoki, Multiple superconducting phases in a nearly ferromagnetic system, *Commun. Phys.* **2**, 147 (2019).
- (12) S. Ran, H. Kim, I.-L. Liu, S. R. Sasa, I. Hayes, T. Metz, Y. S. Eo, J. Paglione, N. P. Butch, Enhancement and reentrance of spin triplet superconductivity in UTe_2 under pressure, *Phys. Rev. B* **101**, 140503 (2020).
- (13) S. M. Thomas, F. B. Santos, M. H. Christensen, T. Asaba, F. Ronning, J. D. Thompson, E.D. Bauer, R. M. Fernandes, G. Fabbris, P. F. S. Rosa, Evidence for a pressure-induced antiferromagnetic quantum critical point in intermediate-valence UTe_2 , *Sci. Adv.* **6**, 8709 (2020).
- (14) G. Knebel, W. Knafo, A. Pourret, Q. Niu, M. Vališka, D. Braithwaite, G. Lapertot, J.-P. Brison, S. Mishra, I. Sheikin, G. Seyfarth, D. Aoki, and J. Flouquet, Field-Reentrant Superconductivity Close to a Metamagnetic Transition in the Heavy-Fermion Superconductor UTe_2 , *J. Phys. Soc. Jpn.* **88**, 063707 (2019).
- (15) A. Rosuel, C. Marcenat, G. Knebel, T. Klein, A. Pourret, N. Marquardt, Q. Niu, S. Rousseau, A. Demuer, G. Seyfarth, G. Lapertot, D. Aoki, D. Braithwaite, J. Flouquet, J. P.

- Brison, Field-Induced Tuning of the Pairing State in a Superconductor, *Phys. Rev. X* **13**, 011022 (2023).
- (16) K. Kinjo, H. Fujibayashi, S. Kitagawa, K. Ishida, Y. Tokunaga, H. Sakai, S. Kambe, A. Nakamura, Y. Shimizu, Y. Homma, D. X. Li, F. Honda, D. Aoki, K. Hiraki, M. Kimata, T. Sasaki, Change of superconducting character in UTe_2 induced by magnetic field, *Phys. Rev. B* **107**, L060502 (2023).
- (17) G. Nakamine, S. Kitagawa, K. Ishida, Y. Tokunaga, H. Sakai, S. Kambe, A. Nakamura, Y. Shimizu, Y. Homma, D. Li, F. Honda, D. Aoki, Superconducting Properties of Heavy Fermion UTe_2 Revealed by ^{125}Te -nuclear Magnetic Resonance, *J. Phys. Soc. Jpn.* **88**, 113703 (2019).
- (18) G. Nakamine, K. Kinjo, S. Kitagawa, K. Ishida, Y. Tokunaga, H. Sakai, S. Kambe, A. Nakamura, Y. Shimizu, Y. Homma, D. Li, F. Honda, D. Aoki, Anisotropic response of spin susceptibility in the superconducting state of UTe_2 probed with ^{125}Te -NMR measurement, *Phys. Rev. B* **103** 100503(2021).
- (19) G. Nakamine, K. Kinjo, S. Kitagawa, K. Ishida, Y. Tokunaga, H. Sakai, S. Kambe, A. Nakamura, Y. Shimizu, Y. Homma, D. Li, F. Honda, D. Aoki, Inhomogeneous Superconducting State Probed by ^{125}Te NMR on UTe_2 , *J. Phys. Soc. Jpn.* **90**, 064709 (2021).
- (20) H. Fujibayashi, G. Nakamine, K. Kinjo, S. Kitagawa, K. Ishida, Y. Tokunaga, H. Sakai, S. Kambe, A. Nakamura, Y. Shimizu, Y. Homma, D. Li, F. Honda, D. Aoki, Superconducting Order Parameter in UTe_2 Determined by Knight Shift Measurement, *J. Phys. Soc. Jpn.* **91**, 043705 (2022).
- (21) Y. Tokunaga, H. Sakai, S. Kambe, T. Hattori, N. Higa, G. Nakamine, S. Kitagawa, K. Ishida, A. Nakamura, Y. Shimizu, Y. Homma, D. Li, F. Honda, D. Aoki, ^{125}Te -NMR Study on a Single Crystal of Heavy Fermion Superconductor UTe_2 , *J. Phys. Soc. Jpn.* **88**, 073701 (2019).
- (22) C. Duan, K. Sasmal, M. B. Maple, A. Podlesnyak, J.-X. Zhu, Q. Si, P. Dai, Incommensurate Spin Fluctuations in the Spin-Triplet Superconductor Candidate UTe_2 , *Phys. Rev. Lett.* **125**, 237003 (2020).
- (23) W. Knafo, G. Knebel, P. Steffens, K. Kaneko, A. Rosuel, J.-P. Brison, J. Flouquet, D. Aoki, G. Lapertot, S. Raymond, Low-dimensional antiferromagnetic fluctuations in the heavy-fermion paramagnetic ladder compound UTe_2 , *Phys. Rev. B* **104**, 100409 (2021).
- (24) D. X. Li, A. Nakamura, F. Honda, Y. J. Sato, Y. Homma, Y. Shimizu, J. Ishizuka, Y. Yanase, G. Knebel, J. Flouquet, D. Aoki, Magnetic Properties under Pressure in Novel Spin-Triplet Superconductor UTe_2 , *J. Phys. Soc. Jpn.* **90**, 073703 (2021).
- (25) K. Kinjo, H. Fujibayashi, G. Nakamine, S. Kitagawa, K. Ishida, Y. Tokunaga, H. Sakai, S. Kambe, A. Nakamura, Y. Shimizu, Y. Homma, D. Li, F. Honda, D. Aoki, Drastic change in magnetic anisotropy of UTe_2 under pressure revealed by ^{125}Te -NMR, *Phys. Rev. B* **105**, L140502 (2020).
- (26) G. Knebel, M. Kimata, M. Vališka, F. Honda, D. Li, D. Braithwaite, G. Lapertot, W. Knafo, A. Pourret, Y. J. Sato, Y. Shimizu, T. Kihara, J.-P. Brison, J. Flouquet, D. Aoki, Anisotropy of the Upper Critical Field in the Heavy-Fermion Superconductor UTe_2 under Pressure, *J. Phys. Soc. Jpn.* **89**, 053707 (2020).

- (27) R. F. Hoyt, H. N. Scholz, D. O. Edwards, Superfluid $^3\text{He-B}$: The dependence of the susceptibility and energy gap on magnetic field, *Physica B+C* **107**, 287-288 (1981).
- (28) Supporting information are available as supplementally materials.
- (29) N. R. Werthamer, E. Helfand, P. C. Hohenberg, Temperature and Purity Dependence of the Superconducting Critical Field, H_{c2} . III. Electron Spin and Spin-Orbit Effects, *Phys. Rev.* **147**, **295** (1966).
- (30) R. H. Heffner, J. L. Smith, J. O. Willis, P. Birrer, C. Baines, F. N. Gygax, B. Hitti, E. Lippelt, H. R. Ott, A. Schenck, E. A. Knetsch, J. A. Mydosh, D. E. MacLaughlin, New phase diagram for $(\text{U,Th})\text{Be}_{13}$: A muon-spin-resonance and H_{c1} study, *Phys. Rev. Lett.* **65**, 2816 (1990).
- (31) S. K. Ghosh, M. Smidman, T. Shang, J. F. Annett, A. D. Hiller, J. Quintanilla, H. Yuan, Recent progress on superconductors with time-reversal symmetry breaking, *J. Phys. Condens. Matter* **33**, 033001 (2020).
- (32) M. Sigrist, T. M. Rice, Phenomenological theory of the superconductivity phase diagram of $\text{U}_{1-x}\text{Th}_x\text{Be}_{13}$, *Phys. Rev. B* **39**, 2200 (1989).
- (33) S. Imajo, Y. Kohama, A. Miyake, C. Dong, M. Tokunaga, J. Flouquet, K. Kindo, D. Aoki, Thermodynamic Investigation of Metamagnetism in Pulsed High Magnetic Fields on Heavy Fermion Superconductor UTe_2 , *J. Phys. Soc. Jpn.* **88**, 083705 (2019).
- (34) A. Miyake, Y. Shimizu, Y. J. Sato, D. Li, A. Nakamura, Y. Homma, F. Honda, J. Flouquet, M. Tokunaga, D. Aoki, Metamagnetic Transition in Heavy Fermion Superconductor UTe_2 , *J. Phys. Soc. Jpn.* **88**, 063706 (2019).
- (35) K. Momma, F. Izumi, VESTA 3 for three-dimensional visualization of crystal, volumetric and morphology data, *J. Appl. Crystallogr.* **44**, 1272-1276 (2011).
- (36) D. Aoki, A. Nakamura, F. Honda, D. Li, Y. Homma, Y. Shimizu, Y. J. Sato, G. Knebel, J.-P. Brison, A. Pourret, D. Braithwaite, G. Lapertot, Q. Niu, M. Vališka, H. Harima, J. Flouquet, Unconventional Superconductivity in Heavy Fermion UTe_2 , *J. Phys. Soc. Jpn.* **88**, 043702 (2019).
- (37) N. Fujiwara, N. Môri, Y. Uwatoko, T. Matsumoto, N. Motoyama, S. Uchida, Superconductivity of the $\text{Sr}_2\text{Ca}_{12}\text{Cu}_{24}\text{O}_{41}$ Spin-Ladder System: Are the Superconducting Pairing and the Spin-Gap Formation of the Same Origin?, *Phys. Rev. Lett.* **90**, 137001 (2003).
- (38) B. Bireckoven, J. Witting, A diamond anvil cell for the investigation of superconductivity under pressures of up to 50 GPa: Pb as a low temperature manometer, *J. Phys. E: Sci. Instrum.* **21**, 841-848 (1998).
- (39) K. Kitagawa, H. Gotou, T. Yagi, A. Yamada, T. Matsumoto, Y. Uwatoko, M. Takigawa, Space Efficient Opposed-Anvil High-Pressure Cell and Its Application to Optical and NMR Measurements up to 9 GPa, *J. Phys. Soc. Jpn.* **79**, 024001 (2010).
- (40) A. Pustogow, Yongkang Luo, A. Chronister, Y.-S. Su, D. A. Sokolov, F. Jerzembeck, A. P. Mackenzie, C. W. Hicks, N. Kikugawa, S. Raghu, E. D. Bauer, S. E. Brown, Constraints on the superconducting order parameter in Sr_2RuO_4 from oxygen-17 nuclear magnetic resonance, *Nature* **574**, 72-75 (2019).

- (41) K. Ishida, M. Manago, K. Kinjo, Y. Maeno, Reduction of the ^{17}O Knight Shift in the Superconducting State and the Heat-up Effect by NMR Pulses on Sr_2RuO_4 , *J. Phys. Soc. Jpn.* **89**, 034712 (2020).
- (42) K. Kinjo, M. Manago, S. Kitagawa, Z. Q. Mao, S. Yonezawa, Y. Maeno, K. Ishida, Superconducting spin smecticity evidencing the Fulde-Ferrell-Larkin-Ovchinnikov state in Sr_2RuO_4 , *Science* **376**, 397-400 (2022).
- (43) K. Kinjo adg2736.zip zenodo (2023).

Acknowledgments:

The authors thank A. Miyake, Y. Yanase, Y. Matsuda, K. Machida, S. Fujimoto, V. P. Mineev, Y. Maeno, S. Yonezawa, J-P. Brison, G., Knebel, W. Knafo for their valuable discussions. This work was supported by the Kyoto University LTM Center.

Funding:

This work was supported by Grants-in-Aid for Scientific Research (Grant Nos.JP19K03726, JP19K14657, JP19H04696, JP19H00646, JP20H00130, JP20KK0061, JP21K18600, JP22H04933, JP22H01168, and JP23H01124).

This work was also supported by JST SPRING (Grant Number JPMJSP2110).

KK, HF, and HM would like to acknowledge the support from the Motizuki Fund of Yukawa Memorial Foundation.

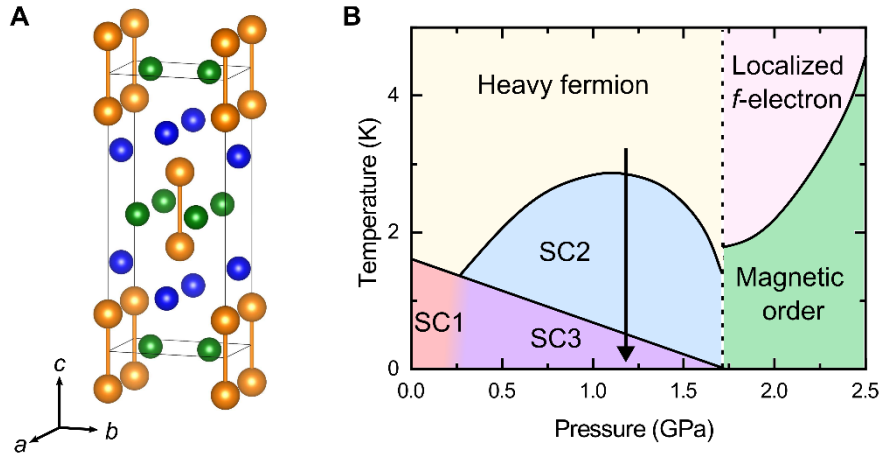


Figure 1. Crystal structure and pressure-temperature phase diagram of UTe₂.

(A) Crystal structure of UTe₂ made by VESTA (35). The U atom forms the dumbbell structure, and the dumbbells form a line along the *a* axis. (B) Pressure–temperature phase diagram of UTe₂. Bold lines correspond to the thermodynamic phase transitions detected by the specific-heat measurements (11, 13). The phase boundary between SC1 and SC3 has not been detected. The arrow represents the measurement range in this report.

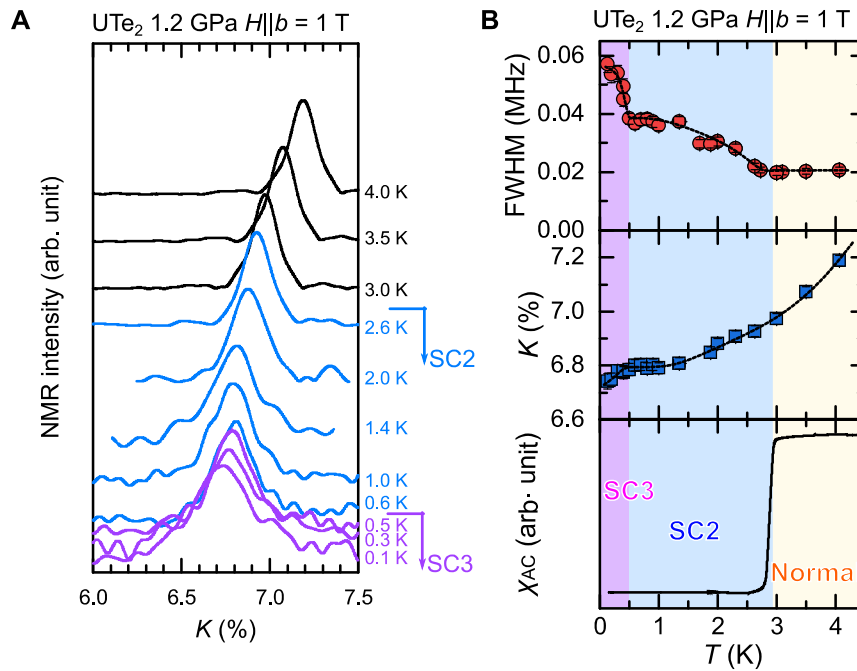


Figure 2. NMR evidence for superconducting-spin rotation.

(A) Temperature variation of the NMR spectra of UTe_2 at 1.2 GPa. (B) Temperature dependence of the full-width half-maximum (FWHM), peak position K of Te2 signal, and χ_{AC} at 1.2 GPa. Line colors in panel (A) and background color in panel (B) represent the phase appearing in Fig. 1(B). The kinks in the T dependence of K and FWHM suggest the phase transition at around 0.5 K, although χ_{AC} does not show any anomaly. The dashed lines in top and middle panels are guides to eye.

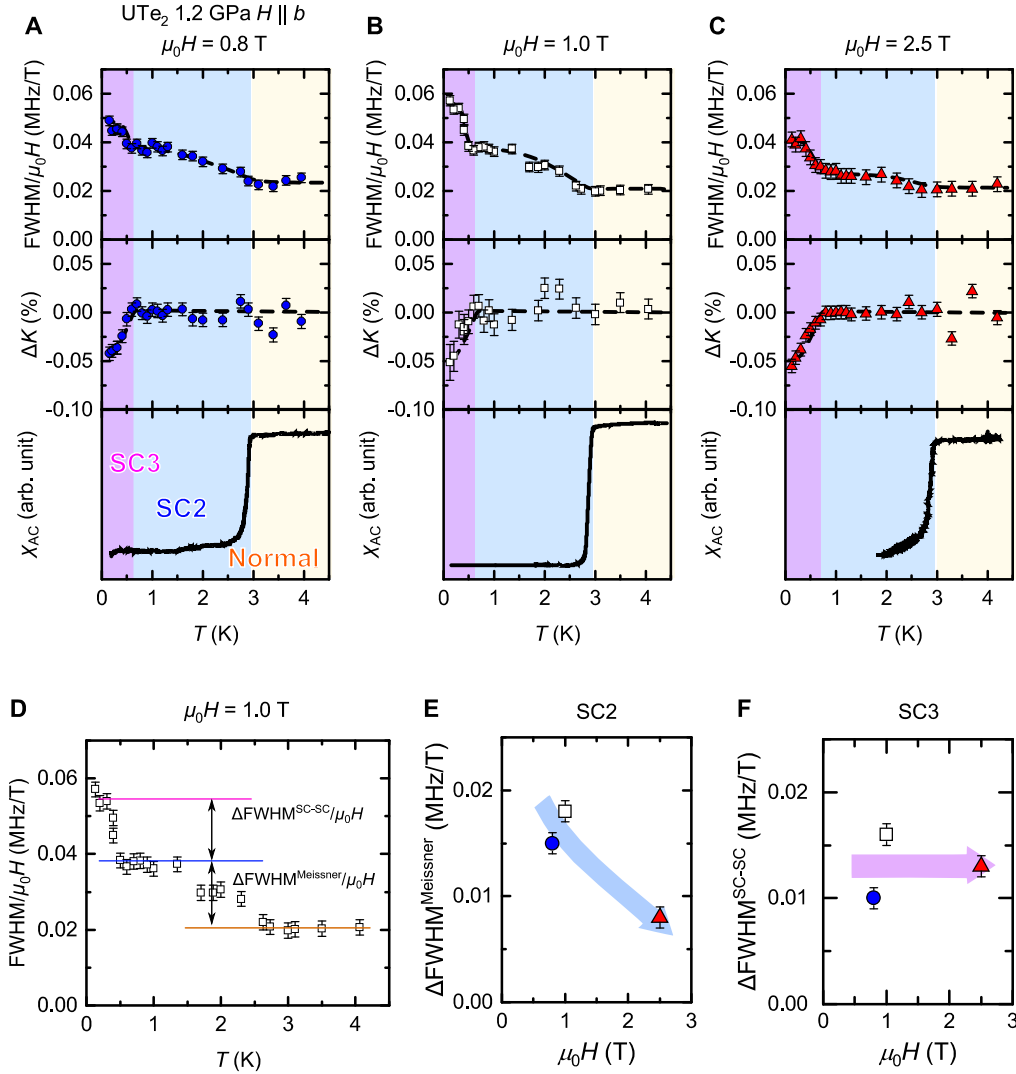


Figure 3. NMR data evidencing the increase in magnetic inhomogeneity.

Temperature dependence of (Top) the FWHM/ $\mu_0 H$, (Middle) ΔK , and χ_{AC} at (A) 0.8 T, (B) 1.0 T, (C) 2.5 T of the Te2 NMR spectrum. (D) The definition of the $\Delta FWHM^{SC-SC}/\mu_0 H$ and $\Delta FWHM^{Meissner}/\mu_0 H$, which are the NMR linewidth broadening in SC2 and SC3 respectively, is shown. The magnetic field dependence of (E) the $\Delta FWHM^{Meissner}/\mu_0 H$ and (F) the $\Delta FWHM^{SC-SC}/\mu_0 H$. The definitions of these two are given in the main text. $\Delta FWHM^{Meissner}/\mu_0 H$ decreases with applying field. This is conventional superconducting behavior, and evidences the bulk superconductivity in the SC2 state. $\Delta FWHM^{SC-SC}/\mu_0 H$ is almost constant against the field.

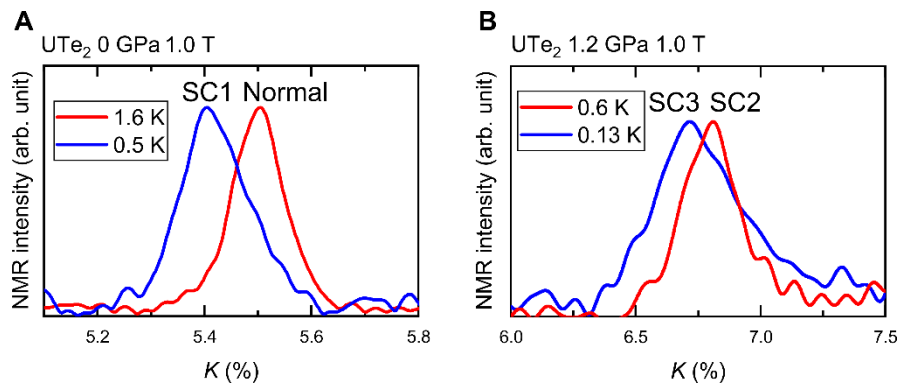


Figure 4. Comparison of the NMR spectrum broadening in SC1 and SC3.

(A) The NMR-spectrum variation occurring in SC1. (B) The NMR-spectrum broadening occurring in SC3. The spectrum in SC3 shows a tail to the larger Knight-shift side than the Knight shift in SC2.

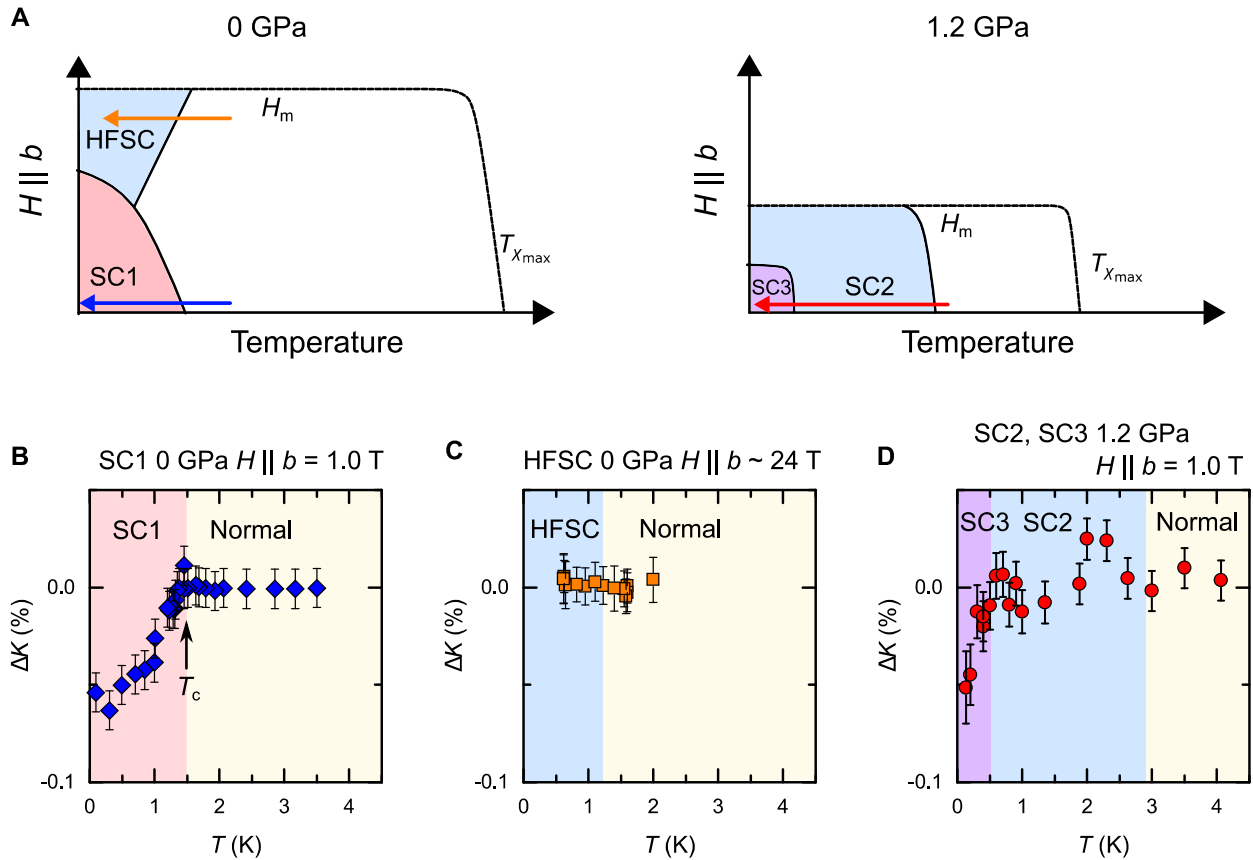


Figure 5. General phase diagram expected from our NMR results.

(A) The schematic images of the H - T phase diagram of UTe_2 at 0 GPa and 1.2 GPa. The bold lines are the transition lines determined by the thermodynamic measurements (11, 13, 15). The dashed line represents the temperature where the χ_b shows maximum ($T_{\chi_{\max}}$) and metamagnetic transition. (B)(C)(D) The temperature dependence of ΔK in 4 states appears in panel (A). The colored arrows in panel (A) represent the measurement range in panels (B,C,D).

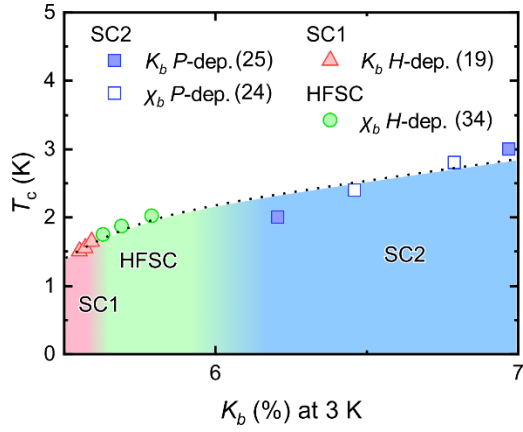


Figure 6. Relation between b -axis susceptibility and critical temperature

This diagram shows relation between b -axis magnetic susceptibility and the T_c of superconducting phases. For K_b between 5.7 and 6.0, T_c is affected by the magnetic field along the b -axis. The extrapolation of T_c to $H = 0$ in HFSC is based on the strong coupling parameter of Miyake *et al* (34). The magnetic field enhances K_b and increases the T_c . As K_b increases further, T_c enters the SC2 region, and when K_b increases to nearly 7%, T_c increases to a maximum of 3 K. The dotted line is guides to eyes.